Controllable Domain Morphology in Coated Poly (lactic acid) Films for High-Efficiency and High-Precision Transporting Water Droplet Arrays

Yongtao Wang[a], Huige Yang*[a], Hongzhi Liu[b], Li Zhang[a], Ruixia Duan[a], Xuying Liu*[a], Jinzhou Chen*[a]

[a] School of Materials Science and Engineering, Zhengzhou University, Zhengzhou 450001, China.

E-mail: cjz@zzu.edu.cn; yanghg@zzu.edu.cn; liuxy@zzu.edu.cn

[b] College of Engineering, Zhejiang Agriculture & Forestry University, Hangzhou, 311300, China

1. Materials

Commercially available PLLA pellets (Ingeo® 4032D) were supplied by Nature Works (Minnetonka, USA). Chloroform, dichloromethane, absolute ethyl alcohol, n-butyl alcohol, and n-butyl acetate were purchased from Tianjin Chemical Regent Co., Ltd. (China) and used as received.

2. Characterization

2.1 Scanning electron microscope (SEM)

The surface morphologies of the as-prepared PLLA surfaces were observed by scanning electron microscopy (SEM, JSM-7500F, Japan) at an accelerating voltage of 5 kV. Prior to the observation, the samples were sputter-coated with a thin layer of gold to avoid the charging.

2.2 Contact angle (CA) and Sliding angle (SA)

Water contact angle values (CAs) were measured by a contact angle meter (JC2000A, Powereach, China) at ambient temperature for each surface. A water droplet of 5 μL water droplets (Microliter syringes, Gaoge, China) was dropped to superhydrophobic coatings. All CAs were measured at five different points and then averaged. Sliding angles (SAs) were measured by setting a substrate to various tilt angles, and then a 5 μL droplet was deposited onto these surfaces from which they instantly rolled off. This angle was defined as water sliding angle (SA). All SAs were measured at five different points and then averaged.

2.3 Adhesive force

The adhesive force was measured using a highly sensitivity micro-electromechanical balance system (Sigma 700/701, Force Tensionmeter, Sweden). A water droplet of 5μL suspending on a hydrophobic metal ring was approached and retracted from the sample's surface at a constant

speed of 2 mm min^{-1} at the ambient environment with a relative humidity of about 35%. The droplet started to move away from the sample surface once contacting, and the balance force gradually increased, and reached the maximum value before the droplet left from the surface. The peak recorded in the force-distance curve was taken as the maximum adhesive force.

2.4 DSC and XRD

Nonisothermal crystallization behavior of the films was studied by differential scanning calorimetry (DSC). During DSC measurement, melt-quenched samples were heated from 30 ℃ to 180 ℃ at a heating rate of 10℃/min in nitrogen gas condition. X-ray diffraction (XRD) patterns were obtained with a Cu Ka radiation (35 kV and 30 mA) at a scanning rate of 4℃/min.

2.5 Micro droplet arrays transporting and device fabrication

The water microdroplet array was prepared by a volume-controllable pipette (0.5-2μL). After the array was prepared well, it was immediately transported onto another one. For the transportation of aqueous conductive ink droplets, a prepatterned source-drain electrode array was already fabricated according to other reports. [1, 2] Then, a 5×5 array was prepared using the same approach on a PLA surface, immediately transported onto the source-drain patterns. The device performance was measured in a semiconductor parameter analyzer (Agilent, B1500A).
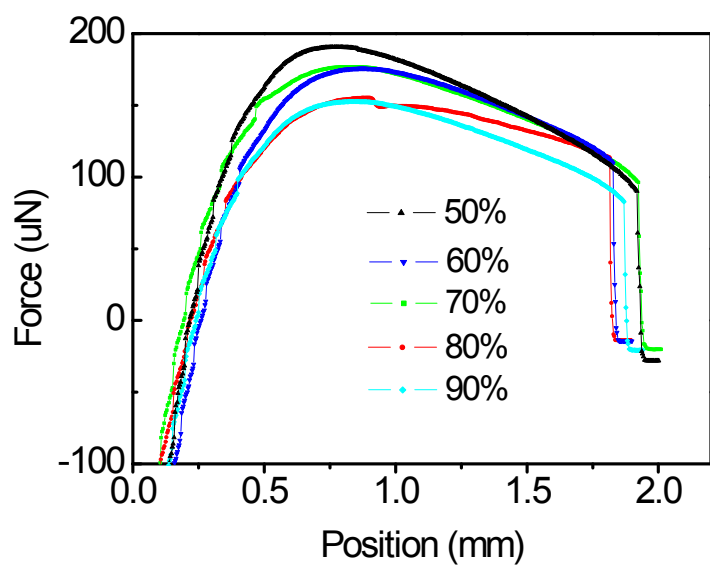
Fig. S1. Force-distance curves of the coating surfaces (before the exfoliation) with various ratio of non-solvent/solvent

Table S1. Solubility and polarity parameters of PLA and the solvents.

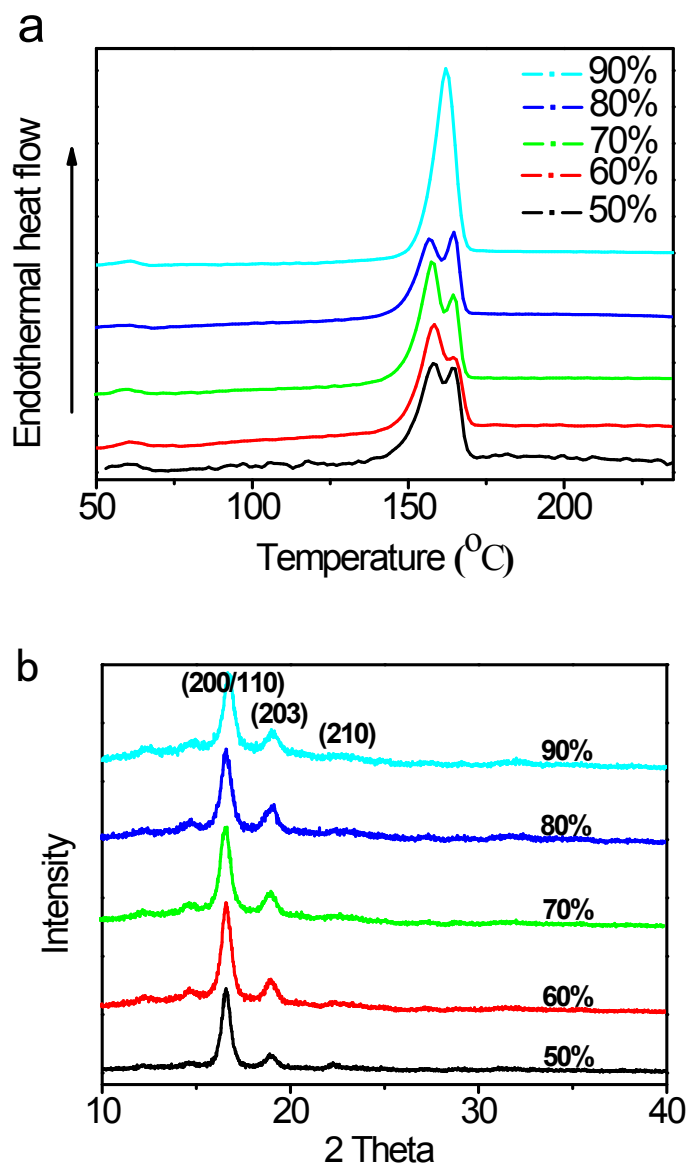| Solvent	Solvent type	δ_d/ MP$^{1/2}$	δ_p/ MP$^{1/2}$	δ_h/ MP$^{1/2}$	δ_t/ MP$^{1/2}$	Boling point (ºC)	Polarity	Viscosity	Relative volatilization rate
PLA	-	17.5	9.5	7.3	21.2	-	-	-	-
TCM	Non-polar	17.8	3.1	5.7	19	61.7	4.4	0.57	-
EtOH	Polar protic	15.8	8.8	19.4	26.6	78.3	4.3	1.08	203
NBA	Polar protic	16	5.7	15.8	23.1	117	3.7	2.95	45
NBAC	Non-polar	15.8	3.7	6.3	17.4	126.5	4	0.68	100

Fig. S2 The crystal analysis of various PLA surfaces. (a) DSC curves, melting enthalpy increases with the volume ratio of non-solvent to solvent, showing higher degree of crystallinity; (b) XRD curves, four crystal forms, including α, β, γ, α', had been reported for PLA depending on different crystallization conditions. As shown in b, the α-form can only be obtained by NIPS process from all samples, indicating the crystal structure has not changed. The diffraction peaks at 2θ= 16.8º, 19.0º, and 22.3º were corresponded to the diffraction peaks at the composite of (200) and (110), the peak of (203), and the peak of (210), respectively.

Table S2. The thermal analysis parameters and mass loss of various samples from Fig. S2a.

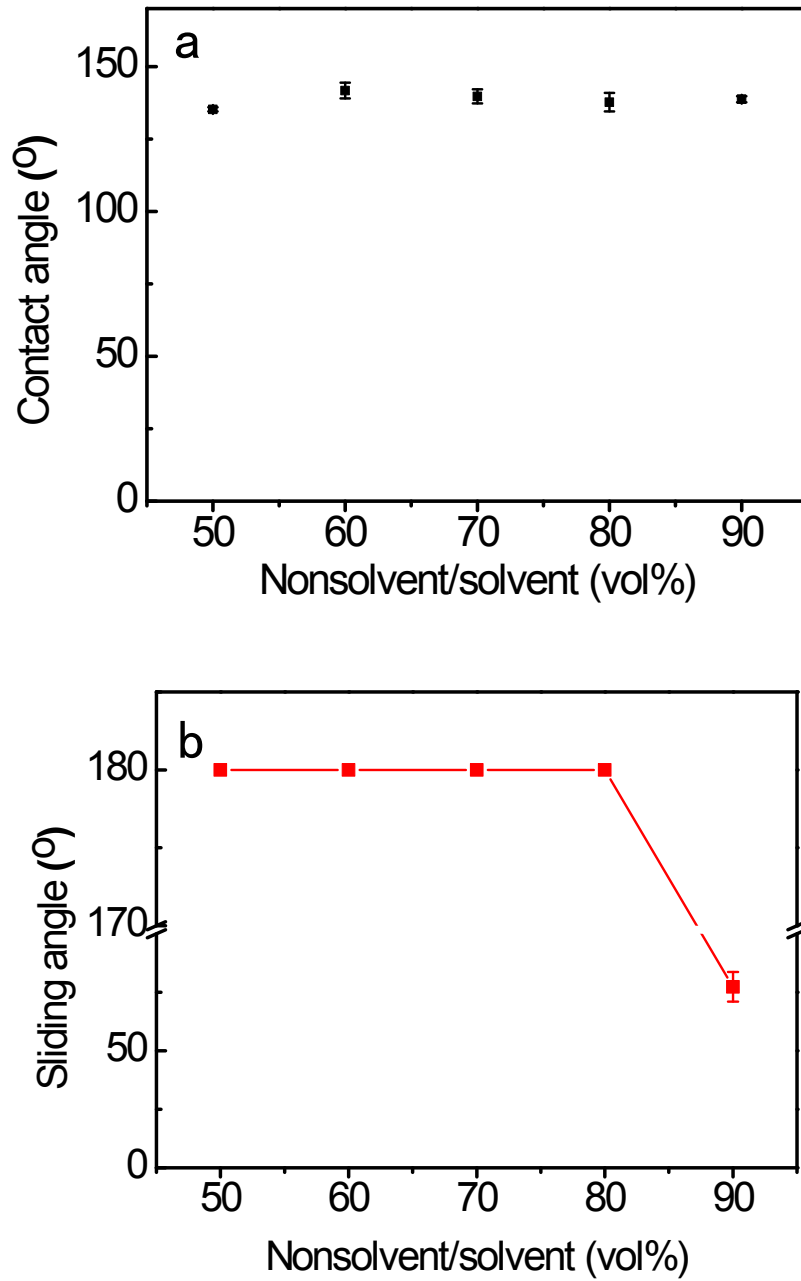| Samples	Glass-Transition Temperature (T_g/℃)	Melting Temperature (T_m/℃)	Melting enthalpy (ΔH_f/J•g⁻¹)	Crystallinity (X_c/%)	Loss (%)
Neat-PLA	57.5	163.5	30.69	33.0	96.01
50%	52.5	158.3	58.01	62.3	96.08
60%	53.6	158.2	54.36	58.4	97.65
70%	55.5	158.4	59.76	64.2	96.19
80%	50.5	165.0	49.66	53.3	99.22
90%	54.2	162.2	66.06	71.0	97.31

Fig. S3 The contact angles (a) and sliding angles (b) on the exfoliated surfaces at the solution evaporation temperature of 50 ℃.
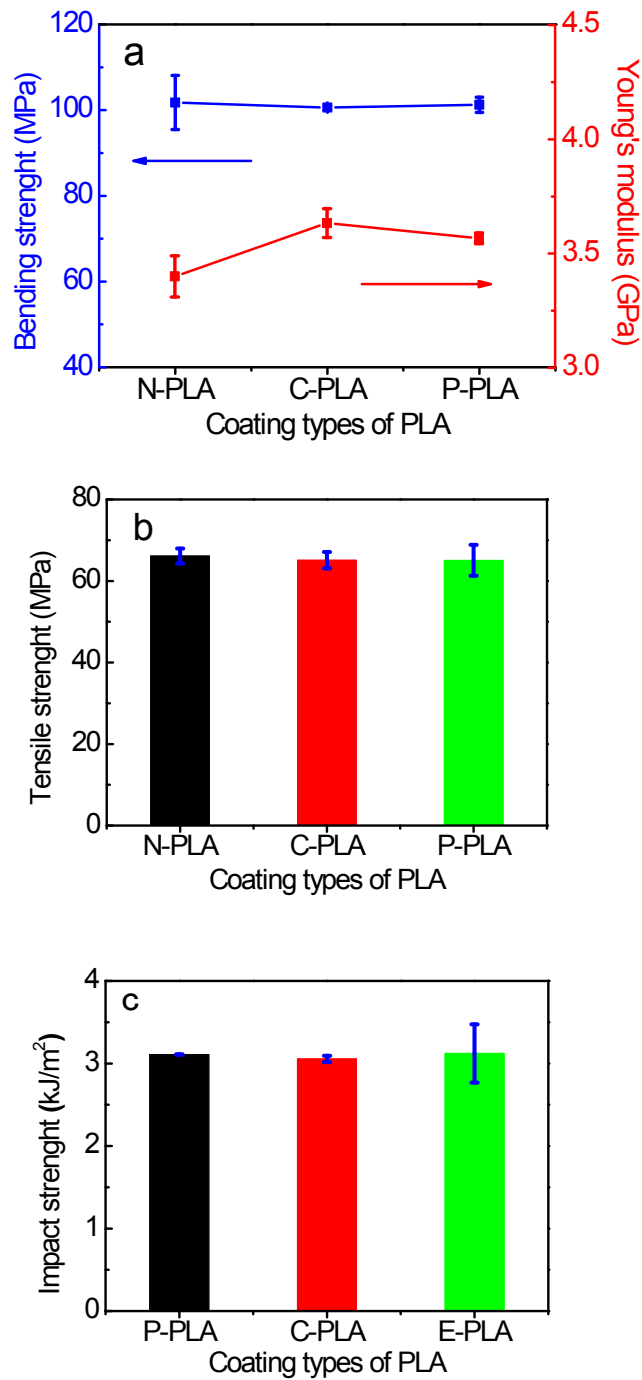
Fig. S4 The mechanical properties for the pristine PLA (P-PLA), coated surface PLA (C-PLA), and exfoliated PLA (E-PLA). (a) Bending strength and Young's modulus; (b) Tensile strength; (c) Impact strength. From the given data, the loss of the mechanical properties of PLA substrates can be ignored, manifesting slight effect on PLA substrates.

Table S3 The mechanical properties of PLA derived from Fig. S6.

Samples	N-PLA	C-PLA	P-PLA
Tensile strength (MPa)	66	65	65
Elongation at break (%)	12.7	12.9	11.3
Impact strength (kJ/m^2)	3.1	3.0	3.1
Bending strength (MPa)	102	101	101
Young's modulus (GPa)	3.4	3.6	3.5

Reference:

1. Liu, X., Kanehara, M., Liu, C., Sakamoto, K., Yasuda, T., Takeya, J., & Minari, T. (2016). Spontaneous Patterning of High‑Resolution Electronics via Parallel Vacuum Ultraviolet. *Advanced Materials*, *28*(31), 6568-6573.

2. Liu, X., Liu, C., Sakamoto, K., Yasuda, T., Xiong, P., Liang, L., Yang, T., Kanehara, M., Takeya, J. and Minari, T., 2017. Homogeneous dewetting on large-scale microdroplet arrays for solution-processed electronics. *NPG Asia Materials*, *9*(7), 409.